Metall. Res. Technol. **116**, 509 (2019)

https://doi.org/10.1051/metal/2018128

Inclusion cleanliness in the metallic alloys
Edited by Jean-Pierre Bellot, Pascal Gardin, Frédéric Gruy

&Metallurgical Research Technology

Available online at:
www.metallurgical-research.org

Regular Article

An assessment of cleanliness techniques for low alloyed steel grades

Aurélie Franceschini[1,*], Fabienne Ruby-Meyer[2], Fabien Midroit[2], Bandiougou Diawara[2], Stéphane Hans[3], Thibault Poulain[3], Cédric Trempont[3], Eric Hénault[4], and Anne-Laure Rouffié[5]

[1] IRT M2P, Metz, France
[2] Ascometal, Hagondange, France
[3] Aubert & Duval, Les Ancizes, France
[4] Datamet, Metz, France
[5] Safran Tech, Magny-les-Hameaux, France

Received: 16 November 2018 / Accepted: 21 November 2018

Abstract. In order to find a method to characterize the inclusion distribution of high-cleanliness materials, complementary techniques were tested, such as high-frequency (80 MHz) ultrasonic testing, X-ray tomography or Extreme Value Analysis (EVA). The micro-cleanliness was also characterized by standard methods based on observations of polished surfaces by light optical or scanning electronic microscopy. The combination of all these techniques, enhanced by metiS software, allows us to determine the complete 3D distribution of oxides or to estimate the probability of largest inclusion size by modelling virtual samples. At the end, fatigue testing was performed in order to try to link fatigue results to previous characterization outcomes.

Keywords: cleanliness / characterization techniques / ultrasonic testing / X-ray tomography

1 Introduction

Steels for the aerospace or automotive industry require enhanced inclusion cleanliness. So-called "high-cleanliness" materials, because of their low volume fraction of inclusions, makes it possible to improve their mechanical characteristics, especially the fatigue life duration, and component weight reduction.

However, the standard methods of characterization seem to have reached their limits to discriminate materials by their level of cleanliness. For instance, the 10 MHz ultrasonic testing, commonly used at the billet or ingot step, can only detect macro-inclusions several hundred of microns in length. Observations of metallurgical sections with an optical or scanning electron microscope make it possible to characterize micro-inclusions ($< 15\,\mu m$) but are not representative enough for the detection of meso-inclusions ($> 15\,\mu m$) due to low detection probability. To complement these observations, these materials are most often characterized by numerous fatigue tests, which offer a true performance indicator on the endurance of future parts. Such tests are long (censoring at 5 or 10.10^6 cycles) and expensive.

For these reasons, alternative inclusion characterization techniques were evaluated. The study focuses on a low alloyed steel air processed with or without a subsequent remelting sequence. The meso-cleanliness was investigated using high-frequency (80 MHz) ultrasonic testing. The micro-cleanliness was characterized by optical and scanning electronic microscopy, combined with image analyses software. This technique has already been successfully used on a very high cleanliness steel [1]. For some typical defects (alignment, meso-inclusion...), additional analyses were carried out: X-ray tomography [2] to precise their shape and EDS to identify their chemical composition. Furthermore, virtual samples, generated with simulation software metiS [3], were investigated to model the most likely inclusion size distribution. This simulation allowed us to estimate the probability of largest inclusion size by Extreme Value Analysis (EVA). Finally, fatigue testing was performed to identify the inclusions responsible for failure. The results were compared with other cleanliness characterization methods for both air melting and remelting process routes.

* e-mail: aurelie.franceschini@irt-m2p.fr

Table 1. Steel composition (wt.%).

C (%)	Si (%)	Mn (%)	Ni (%)	Cr (%)	Mo (%)	V (%)	Al (%)	S (%)
0.30	0.3	0.5	0.2	3.0	0.85	0.3	0.01	<0.001

2 Materials and methods

The studied alloy is a low alloyed steel (see Tab. 1), for which a high cleanliness is required. Several characterization techniques were evaluated for two processing routes – air processing with or without a subsequent remelting sequence – which lead to very different inclusion populations. The steel cleanliness was studied on heat treated rolled bars, with a mechanical resistance $R_m \approx 1300$ MPa.

Light optical microscopy (LOM), combined with image analyser system, is one of the most common method used to evaluate inclusion content of steel. This method is based on the contrast difference between non-metallic inclusion and the ferrous matrix. Its main advantage is to perform fast automated measurements, even for large field observations. Although, it does not enable to identify the composition of inclusions, it makes it possible to sort inclusions by types (sulphide, oxide or nitride) according to grey level difference, size and morphology. In the frame of this study, LOM was performed on fields with area of 5000 mm^2 to establish the inclusion density, with a detection limit of 3 µm.

The inclusion characterization was also performed using field emission gun scanning electron microscopy (FEG-SEM), combined with energy dispersive spectroscopy (EDS) and image analyser system. The identification of inclusions is based on the contrast difference between non-metallic inclusion and the ferrous matrix. This method enables also to dissociate oxides from nitrides or sulphides by grey level difference. Then this technique makes it possible to evaluate the composition of inclusions with EDS analyses. Two measurement conditions were used for this study: a) detection limit of 0.5 µm on 50 mm^2 area; b) detection limit of 3 µm on 200 mm^2 area.

Ultrasonic (US) testing is a non-destructive technique based on the propagation of ultrasonic waves in the tested material. An ultrasound transducer connected to a computer is passed over the object being inspected. Reflected ultrasounds come from an interface, such as the back wall of the object or from an imperfection, like an inclusion, within the object. The computer displays a signal with an amplitude, representing the intensity of the reflection, and the arrival time, representing the distance from the surface. For this study, frequency of 80 MHz was used in order to detect reflectors of more than 20 µm equivalent diameter on an acoustic microscope SAM 301 from PVA Tepla. This technique is applied on bearing steels for many years, and well described in [4]. The analysis was performed on samples after: a) annealing heat treatment (700 °C for 34 h), in order to reduce reflections of US signal due to the microstructure; b) polishing step ($Ra < 0.2$ µm), in order to avoid reflections due to the roughness of surface. The volume analysed per sample was about 10 cm^3.

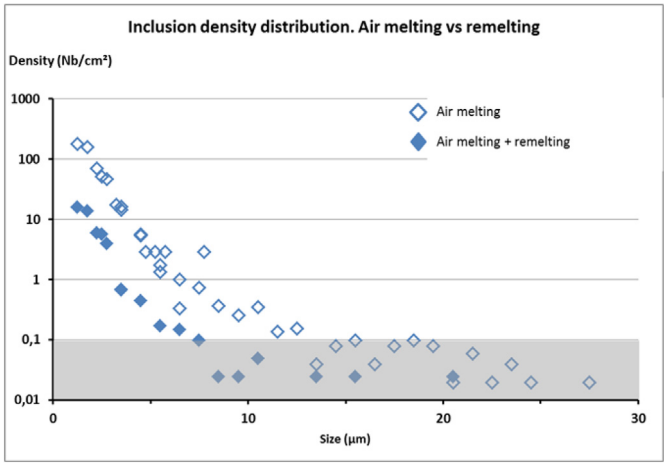

Fig. 1. Comparison of inclusion density distribution for inclusion size > 0.5 µm for both samples (grey area: imprecise values due to an insufficient surface area analysis for inclusion density measurement).

Additional analyses were performed on some particular defects detected by ultrasonic testing (alignment, large isolated particle). First, X-ray tomography [2] was investigated on $3 \times 3 \times 10$ mm^3 samples on a phoenix v|tome|x s X-ray system at INSA Lyon. For the purposes of the study, the voxel size was set to 2 µm, which is sufficient for the observation of inclusion size of 10–20 µm. The volume analysed per sample was about 0.027 cm^3. Then, for the alignment, the sample was polished until it was revealed at the surface. The alignment was thus characterized by SEM and EDS analyses.

Fatigue tests were performed to identify the inclusions responsible for failures in each process route. The fatigue specimens were taken cross-wise on rolled bars. Considering the diameter of the bars, the gage part was perfectly centred on the core of the product. The specimens had a gage length measuring Ø5.6 mm × 16 mm, which corresponds to a volume of 0.4 cm^3. The tests were carried out on hydraulic machines with imposed stress with a load ratio $R_\sigma = 0.1$ and a frequency of 50 Hz. Tests are stopped after 5.10^6 cycles. The test conditions were chosen to explore both the behaviour near the fatigue limit, and the behaviour at higher stress levels. For each specimen, a fracture surface analysis was performed using a conventional SEM combined with an EDS sensor. The initiation zone was observed and analysed to determine the size and the chemistry of the inclusion(s) at the origin of the fracture. Nearby inclusions were also characterized.

3 Results

3.1 Micro-cleanliness

The Figure 1 shows the inclusion numerical density distribution for both processes. The inclusion density distribution varies from several decades depending on the size of the inclusions and the level of cleanliness associated with the production process. This figure reveals also that, even with an analysed area of 5000 mm^2, microscopy is not

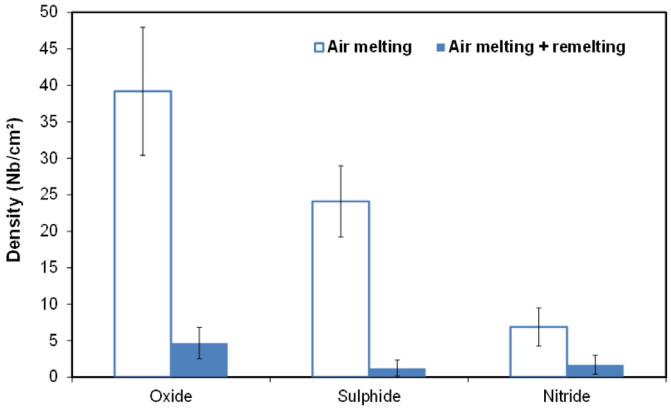

Fig. 2. Inclusion repartition by nature.

Table 2. Inclusion composition evaluated from SEM-EDS analyses.

	Air melting	Air melting + remelting
Inclusion composition (SEM-EDS measurements)	Al_2O_3–MgO Al_2O_3 with MgO > 30% Isolated CaS–MnS Some TiN	Al_2O_3–MgO Some CaS Some TiN

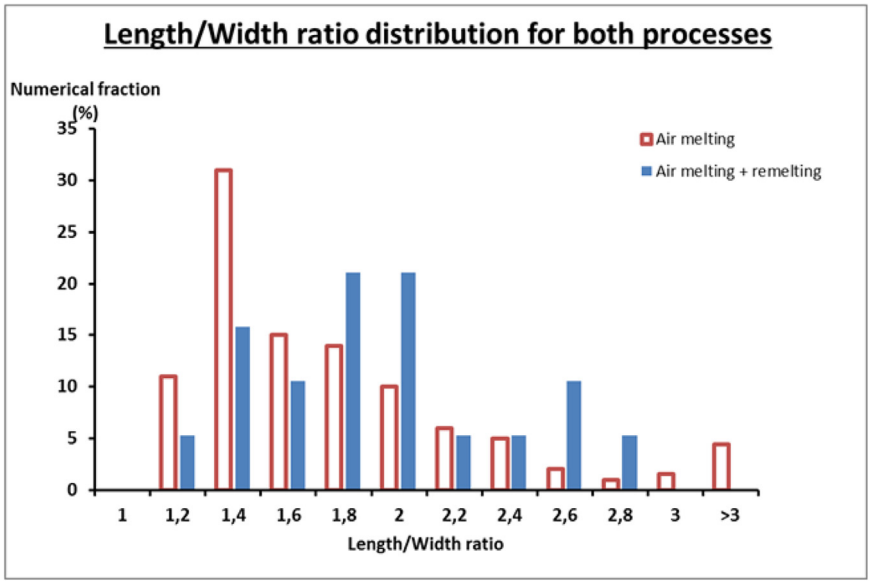

Fig. 3. Comparison of length/width ratios for both processes.

sufficient to obtain reliable values for inclusion size above 10 µm.

Whatever the process, oxides are the main population of inclusions (Fig. 2). The oxides of the remelting processed sample are essentially spinel-type oxides (Al_2O_3–MgO), whereas there are also magnesia-rich oxides (Al_2O_3 with MgO > 30%) after air melting (Tab. 2).

Sulphides and nitrides are present significantly only on the sample resulting from air processing, at levels 2 to 5 times lower than for the oxides. Sulphides are composed of a mixture of MnS and CaS for the air processed sample, and only CaS for the remelting. Some TiN were found on both processes (Tab. 2).

Image analysis also provides information on the morphology of inclusions. Figure 3 shows the distribution of the length/width ratios for each process on rolled bars. It can be noted that the l/L ratios are centred on 1.4 (rather spherical inclusions), with a maximum ratio of 5.3 for the air processed sample. For remelting processed sample, the distribution of this ratio is more spread out, with values mainly between 1.4 and 2.6, but with no value above 3.

3.2 Meso-cleanliness

The objective is to look for inclusions larger than those characterized in the previous chapter. With ultrasonic testing at 80 MHz, inclusions larger than 20 µm should be detected [4]. Examples of C-scan for each process are presented in Figure 4. With a quick visual analysis, one immediately notices a significant difference in inclusion numerical density between each sample.

The comparison of reflector density distribution confirms that there are 15 to 20 times fewer reflectors for remelting processed sample (Fig. 5). Moreover, three alignments, from 0.25 to 0.75 mm length, were found in the air processed sample but none after remelting process. In

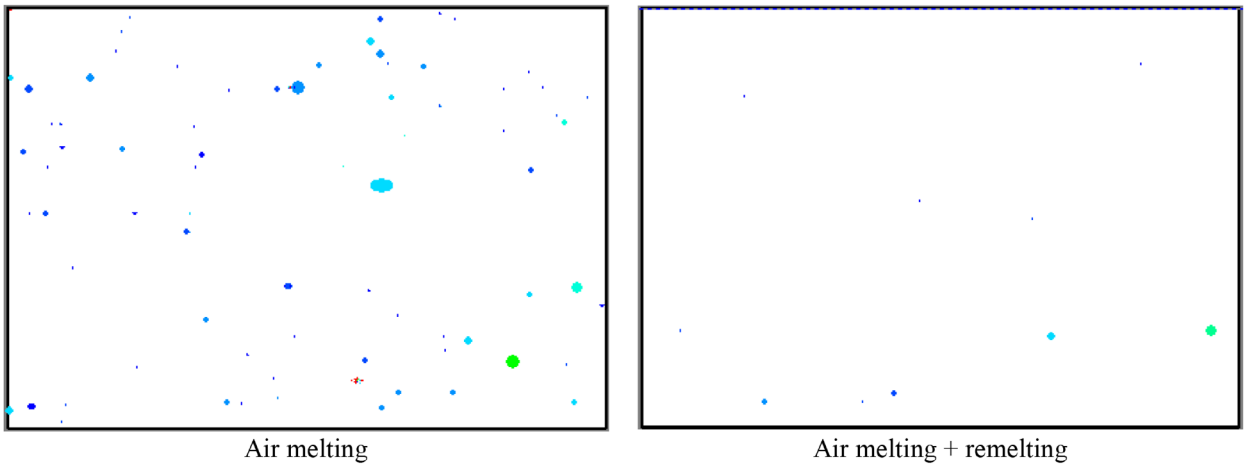

Fig. 4. Example of C-scan map for each sample.

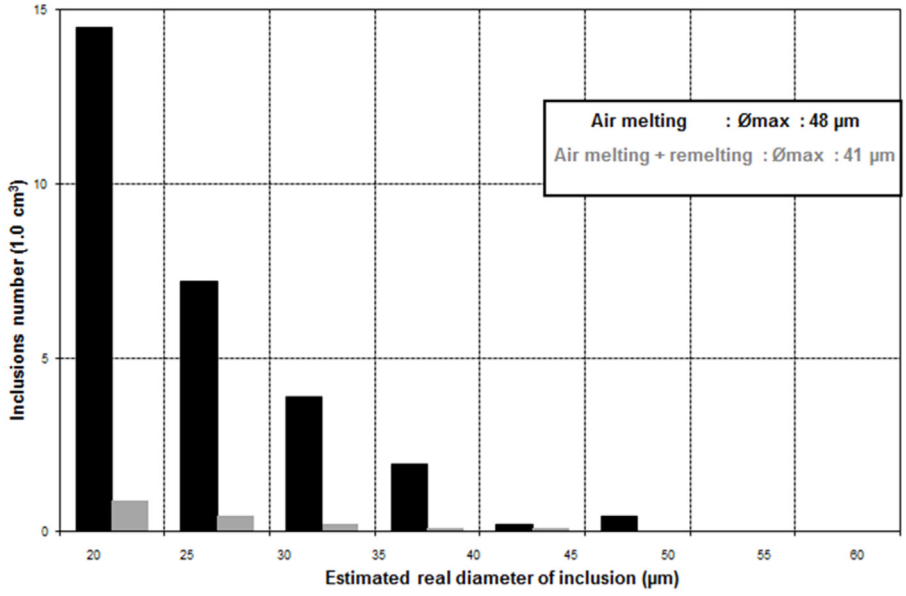

Fig. 5. Comparison of reflector density distribution for both samples above 20 µm.

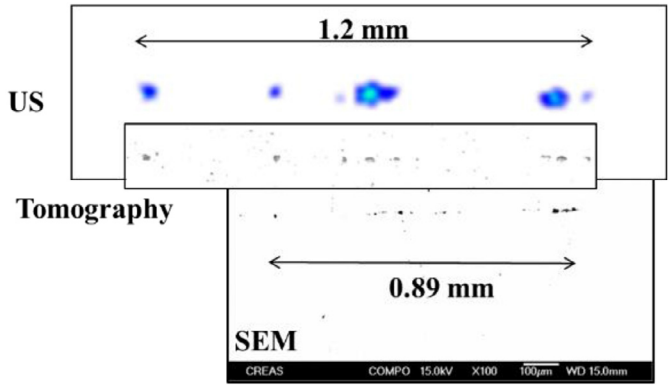

Fig. 6. Detection of an alignment in air processed sample by three techniques: US 80 MHz, X-ray tomography and SEM.

the inspected volume, the largest reflector has an equivalent diameter of 48 µm for air processed sample, not far from the one from remelting processed sample (41 µm).

3.3 Additional analyses on typical defects

Due to their particular composition (mainly calcium aluminate-based oxides), some big inclusions in the as-cast stage could be sufficiently stretched by the rolling step to form an alignment [5]. In order to study an alignment from air processed sample, a tomography test specimen was prepared following the protocol presented in Section 3. The C-scan of the studied alignment is in Figure 6. The length of the alignment is estimated to 1.2 mm; however, it is difficult to estimate the size of the inclusions composing it,

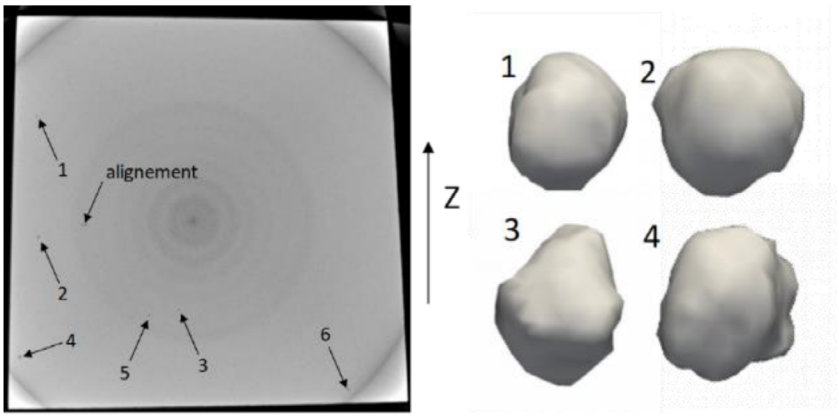

a) Location of inclusions in XY section of the specimen

b) Volume reconstruction of 4 globular inclusions

Fig. 7. Location and volume reconstruction of an alignment and globular inclusions from air processed sample.

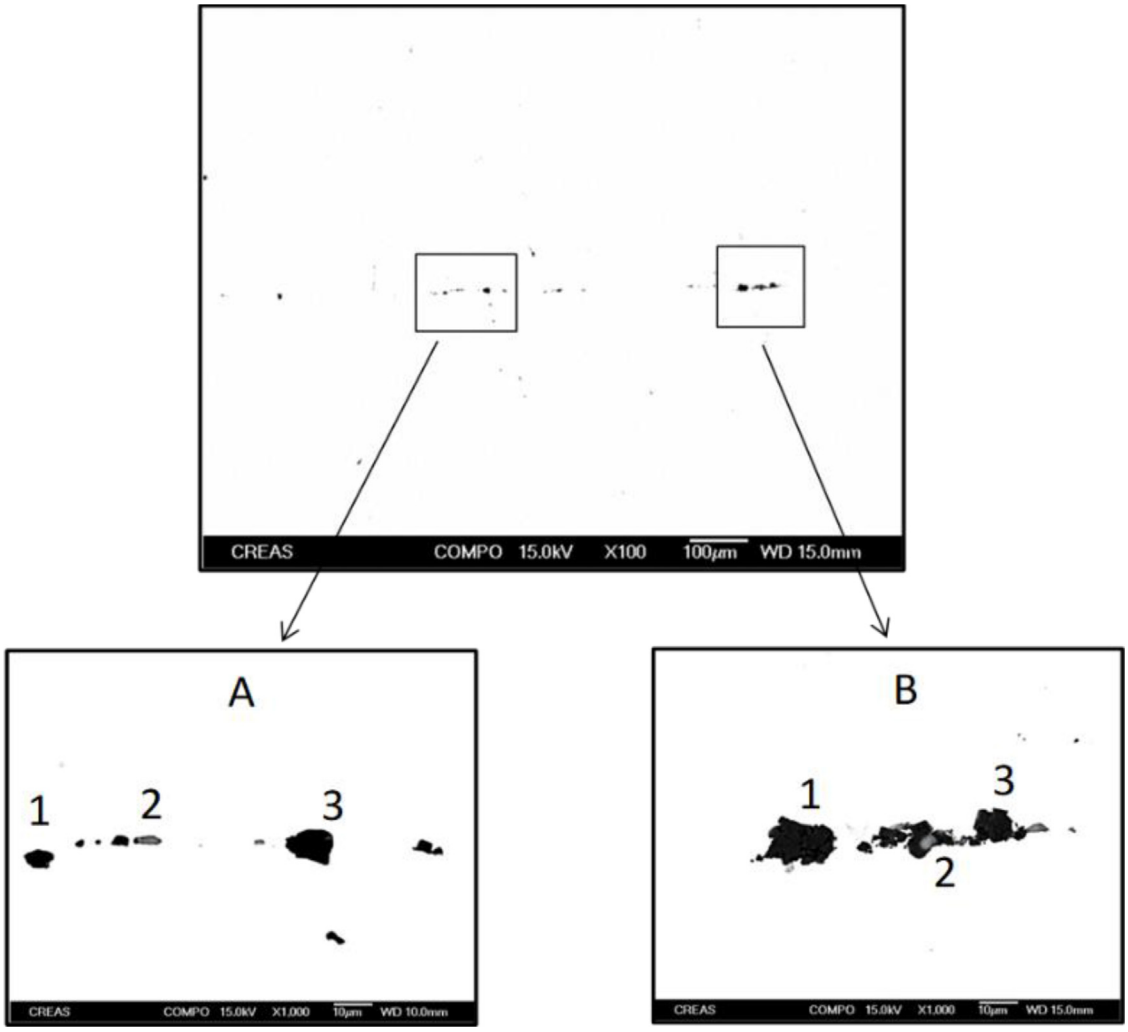

Fig. 8. Micrographic observation of the alignment and focus on two particular areas.

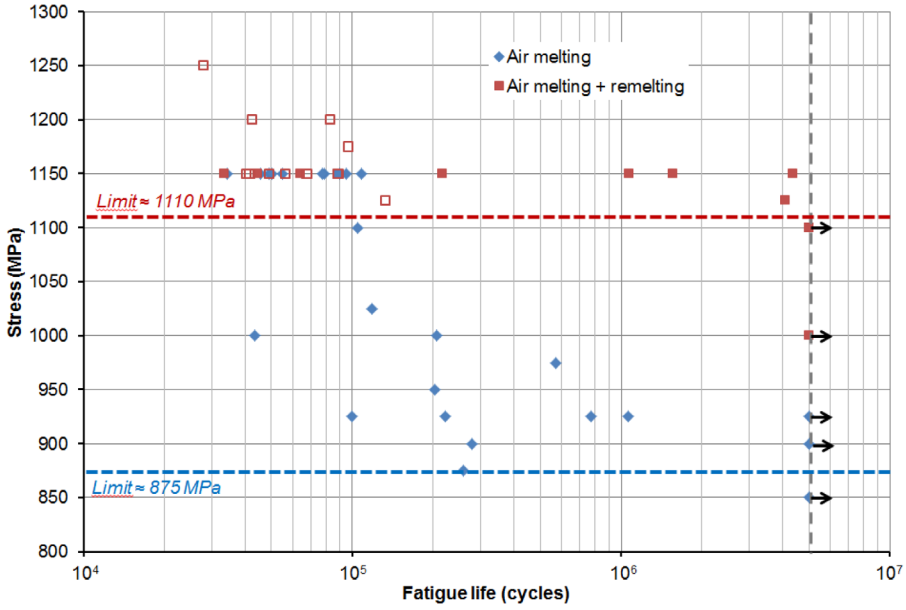

Fig. 9. Fatigue life plots for air melting and remelting process. The empty squares on the graph represent the crack initiation sites on notch. The squares on the right side (with arrow) correspond to specimens that did not break after 5.10^6 cycles.

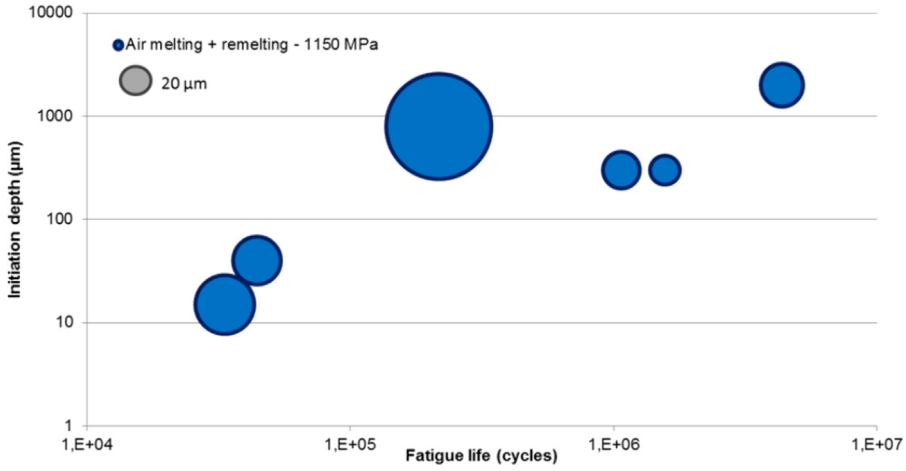

Fig. 10. Influence of location and size of initiation area on the fatigue life.

since the multiple reflectors can amplify the detected signal.

On the XY section of the specimen observed by tomography, we notice the presence of 6 inclusions in addition to the alignment (Fig. 7a). The globular inclusions were not detected by high frequency ultrasound because of their location in the specimen. Indeed, only the volume between 0.4 and 0.9 mm deep is probed. The volume reconstruction of the 4 largest inclusions is in Figure 7b; they have an equivalent diameter between 15 and 20 µm.

The alignment was difficult to locate because of a very low signal-to-noise ratio. The volume reconstruction of this alignment is in Figure 6. It consists of very small inclusions, from 5 to 15 µm equivalent diameter.

After analysing by X-ray tomography, the specimen was polished until the alignment is revealed at the surface for SEM observations. In the polishing surface, the visible part of the alignment is slightly less than 900 µm (Fig. 8). The alignment consists of fragmented particles, the largest of which has an apparent diameter of 16 µm in the polishing surface.

The Figure 6 shows the comparison of detection of the same alignment by US 80 MHz, X-ray tomography and SEM.

3.4 Fatigue testing

Fatigue testing is mainly carried out for two purposes:
– identify or check the mechanical behaviour of a given material;
– characterize the inclusion cleanliness of a material.

Both manufacturing processes have significantly different fatigue limits resulting from different levels of inclusion cleanliness (Fig. 9). However, for high stress levels

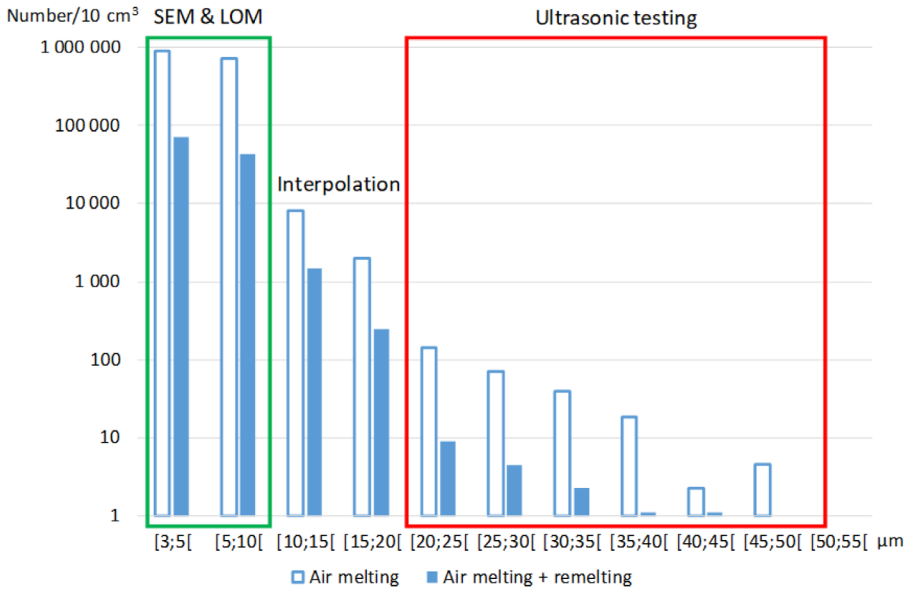

Fig. 11. 3D oxide density distribution modelled with metiS software.

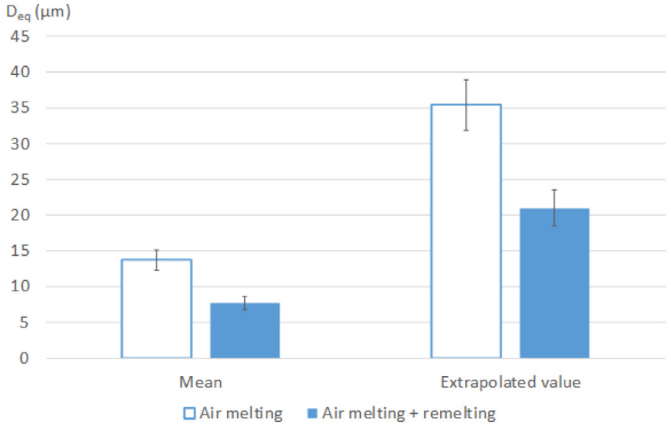

Fig. 12. Mean and extrapolated value issued from extreme values analyses: Mean: mean of 100 virtual measures on 24 areas of 150 mm^2; Extrapolated value: extrapolated value for A = 100 000 mm^2.

(≈1150 MPa), the different processes seem to converge towards a single curve.

The results demonstrate a clear effect of inclusion cleanliness depending on the stress level. This evolution is explained by the relative importance of the initiation and propagation phases according to the applied stress level:
– at low stress level, initiation is an important part of the specimen life and the characteristics of the defect (internal or on surface, small or large inclusion) therefore plays a predominant role over the obtained lifetime;
– at high stress level, the initiation is fast and the specimen life is mainly lead by the propagation phase, which is independent of the type of initiation site considered.

The specimen fatigue-life is mainly controlled by the distance between the initiation area and the free surface (Fig. 10). If the initiation area is close to specimen edge, the presence of the free surface will accelerate the propagation of crack. This influence of the edge is often considered by using the notion of "fish-eye", which corresponds to a zone of different aspect compared to the rest of the facies of rupture, all around the initiation area. If the fish-eye is complete and is not in contact with the surface, the fatigue life is controlled by inclusion size.

The main difference between the two processes is the size of the defects that initiate the failure:
– about 5 to 15 µm isolated particles and large alignments larger than 100 µm for the air-process;
– only isolated particles from 10 to 20 µm for the remelting process.

The chemistry of inclusions present at fracture area is similar for both processes, mainly with particles composed of alumina and magnesia.

The sharp decrease of oxide density (especially for inclusion larger than 10 µm) obtained with the remelting process (see Fig. 11) is well correlated with the subsequent increase (+25%) of fatigue life.

3.5 Complete oxide size distribution

On the basis of the inclusion size distributions, measured by microscopy (LOM + FEG-SEM) and ultrasonic testing (80 MHz), a complete oxide size distribution was calculated using Datamet's metiS software [3]. A 3D size distribution was modelled based on 2D analyses (LOM + FEG-SEM) for 3–10 µm inclusion range and on 3D analysis (US 80 MHz) for inclusion larger than 20 µm. The intermediate size range was interpolated to evaluate the final 3D size distribution in the range 3–50 µm. Due to this interpolation, the oxide size distribution between the 3–50 µm can be obtained for each production route. It is plotted on Figure 11.

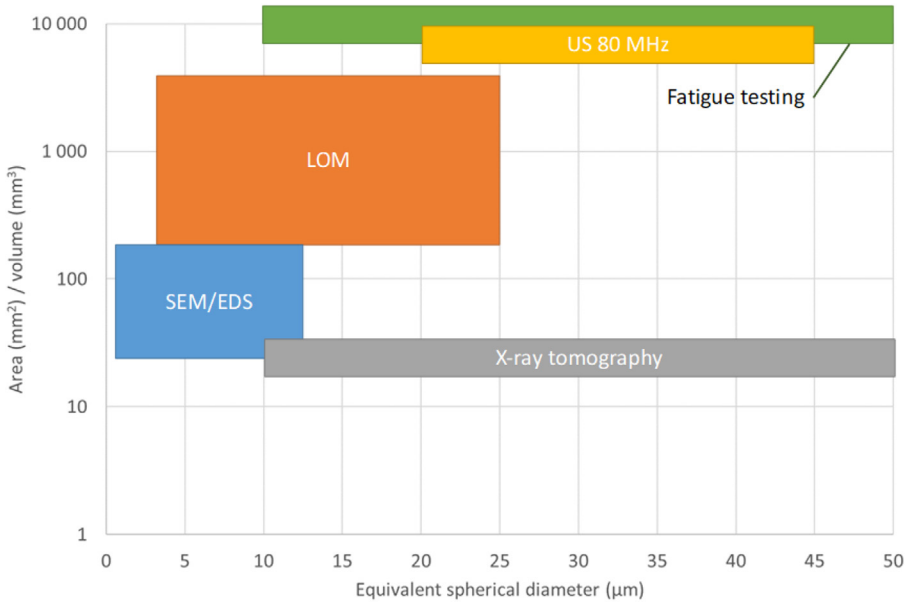

Fig. 13. Schematic representation of inclusion measurements methods depending on inclusion size and inspected area or volume of the sample.

3.6 Statistics of extreme values

Extreme value analysis is a statistical method to estimate the most likely maximum size of inclusion in steel. It requires the preparation of numerous polished samples, which is time consuming. To overcome these difficulties, virtual 3D samples were conceived based on the inclusion density distribution obtained by different methods (SEM, LOM and US). Based on ASTM E2283 standard and with the help of metiS software, 24 virtual areas of 150 mm^2 were created, and these measurements were repeated 100 times. The extrapolated values for the largest inclusion in 100 000 mm^2 area are 35 ± 4 µm diameter for air processing, and $21\,\mu m \pm 4\,\mu m$ diameter for the remelting process (Fig. 12). These estimated values are close to the maximum size of reflection detected with the US-80 MHz method (50 µm for air processing and 35 µm for the remelting process) and to the typical size revealed by fatigue testing (up to 20 µm for isolated particles).

4 Discussion

The characterization work focused on a low alloyed steel grade produced by two different processes (air-cast, air-cast + remelting sequence). These two production routes lead to two different levels of cleanliness. This allowed to compare in a relevant way the potentialities of each method of characterization according to the level of cleanliness.

The Figure 13 is a schematic representation of inclusion measurements methods, representing the size range of detected inclusion depending on the area or volume of inspection. All techniques are complementary to characterize the whole distribution of inclusions.

X-ray tomography provides additional information to conventional techniques, such as the shape and location in volume of inclusions. However, it requires a lot of time to prepare samples and data processing to reconstruct the images, and defects to characterize should be detected by another technique. Therefore, it cannot be substituted to techniques such as SEM or high frequency US.

In Figure 11, it is noticeable that the inclusion density distribution varies from several decades depending on the size of the inclusions and the level of cleanliness associated with the production process. It is therefore necessary to adapt the analysis surface or volume accordingly. The metiS software enables to estimate the variability of each measurement method. Tables 3 and 4 below summarize the estimation of the minimum area or volume required to observe one inclusion, based on size and process route.

As demonstrated in these tables, an analysed surface of 1000 mm^2 is suitable for evaluating the cleanliness of air processed samples up to 10 µm, while for remelting processed samples an area of 5000 mm^2 is necessary. Therefore, there is an interest in increasing the area of analysis (large fields method) to better quantify the occurrence of large inclusions or to analyse high-cleanliness processes. Likewise, for ultrasonic testing, an analysed volume of 10 cm^3 is appropriate for evaluating the cleanliness in the range 20–50 µm of the air processed samples but does not allow to obtain representative measurements on remelting processed samples for inclusions larger than 30 µm.

The metiS software enables also to calculate the amount of oxygen associated with the oxides measured in the 0.5–50 µm range and compares it with the value of total oxygen measured by combustion (Tab. 5). This inclusion oxygen content represents approximately 50–70% of the total oxygen content for air processing. For the remelting process, this ratio becomes very low (less than 20%). It is likely that for the remelting process, a large part of the oxygen remains in dissolved form or at most

Table 3. Estimation of the minimum area required to observe one inclusion (mm^2).

Equivalent diameter (μm)	Air melting	Air melting + remelting
3	5	50
5	50	250
10	250	2000
15	1000	5000
20	2500	15 000

Table 4. Estimation of the minimum volume required to detect one inclusion (mm^3).

Equivalent diameter (μm)	Air melting	Air melting + remelting
3	0.005	0.05
5	0.05	0.5
10	1	10
15	10	100
20	50	500
30	500	10 000

precipitates in the form of very small oxides, less than 0.5 μm. This is why the estimated amount of the inclusion oxygen based only on the amount of oxides larger than 0.5 μm length is largely lower than the total oxygen measured by combustion. The total oxygen content is therefore not a relevant indicator for determining the cleanliness level in this case.

Both manufacturing processes have significantly different levels of inclusion cleanliness, resulting in different fatigue limits. For high stress levels, the different processes seem to converge towards a single curve.

The main differences between the two processes with regard to fatigue resistance are:

- the size of the inclusions that initiate the failure: a few microns for air processed samples; mainly from 10 to 20 μm on remelting processed samples;
- alignment structure: for air processed samples, continuous alignment of particles; for remelting processed samples, particles on the same axis but rather far apart from each other.

Both processes lead to different distribution populations for oxides from 0.5 to 10 μm. However, the chemistry of the inclusions is very similar for the two processes, mainly with particles composed of alumina and magnesia.

5 Conclusion

Two steel production routes, air melting with or without a subsequent remelting sequence, were investigated using various inclusion characterisation techniques. Each technique fitted an inclusion size range and, depending of cleanliness level, characterisation area or volume should be adapted to be representative. X-ray tomography could give some inputs on shape and relative position of inclusions, but only on defects previously identified by another technique. Modelling allowed reconstruction of the 3D distribution of the inclusion sizes measured by each technique. It also enabled estimating variability of each technique. Virtual Extreme Value Analysis enabled estimating the largest inclusion potentially present in the alloy. The improvement in fatigue resistance (+25%) was consistent with the level of cleanliness, greatly improved by the remelting process. Fracture surface analysis of fatigue specimens provided additional information with respect to the above techniques, in particular the failure sensitivity associated with the presence of small particle alignments. In conclusion, all techniques used in this study were complementary to evaluate the cleanliness of melts. Conventional techniques made it possible to discriminate between two different process routes but fatigue testing remains the most sensitive method to measure the quality of a product.

Table 5. Comparison between measured total oxygen content and estimated oxygen content from oxide inclusions > 0.5 μm.

	Air melting (ppm)	Air melting + remelting (ppm)
Total oxygen content (measured)	6	4
Estimated oxygen content from calculated oxides density distribution obtained by SEM measurements (oxide > 0.5 μm)	4	0.5

Acknowledgements. This research is part of the ELABORATION project coordinated by the Institut de Recherche Technologique Matériaux Métallurgie et Procédés (IRT M2P), with the support of Agence Nationale de la Recherche (ANR). The authors wish to thank the industrial partners, Ascometal, Aubert & Duval and Safran, for their work with the samples and metallographic analyses, and the Datamet society for assistance with the calculations on metiS software.

References

1. G. Jeanmaire, M. Dehmas, A. Redjaïmia, S. Puech, G. Fribourg, Precipitation of aluminum nitride in a high strength maraging steel with low nitrogen content, Mater. Charact. **98**, 193–201 (2014)
2. A. Stiénon, A. Fazekas, J.-Y. Buffière, A. Vincent, P. Daguier, F. Merchi, A new methodology based on X-ray micro-tomography to estimate stress concentrations around

inclusions in high strength steels, Mater. Sci. Eng. A **513–514**, 376–383 (2009)
3. E. Hénault, Comparison of inclusion assessment rating standards in terms of results and reliability by numerical simulation, J. ASTM Int. **7(3)**, 1–11 (2010)
4. F. Midroit, F. Merchi, M. Meheux, Non metallic inclusion density in bearing steel characterized by ultrasonic testing, in: J.M. Beswick (Ed.), Bearing Steel Technologies: 10th Volume, Advances in Steel Technologies for Rolling Bearings, STP1580, ASTM International, West Conshohocken, PA, 2015, 116 p.
5. G. Bernard, P.V. Riboud, G. Urbain, Étude de la plasticité d'inclusions d'oxydes, Rev. Metall. CIT **78(5)**, 421–434 (1981)

Cite this article as: Aurélie Franceschini, Fabienne Ruby-Meyer, Fabien Midroit, Bandiougou Diawara, Stéphane Hans, Thibault Poulain, Cédric Trempont, Eric Hénault, Anne-Laure Rouffié, An assessment of cleanliness techniques for low alloyed steel grades, Metall. Res. Technol. **116**, 509 (2019)